PAPER

Check for updates

Short oligopeptides with three cysteine residues as models of sulphur-rich Cu(I)- and Hg(II)-binding sites in proteins†

Edit Mesterházy, [ab] Colette Lebrun, [b] Serge Crouzy, [c] Attila Jancsó (ID) *[b] and Pascale Delangle (ID) *[a]

The essential Cu(I) and the toxic Hg(II) ions possess similar coordination properties, and therefore, similar cysteine rich proteins participate in the control of their intracellular concentration. In this work we present the metal binding properties of linear and cyclic model peptides incorporating the three-cysteine motifs, CxCxxC or CxCxC, found in metallothioneins. Cu(I) binding to the series of peptides at physiological pH revealed to be rather complicated, with the formation of mixtures of polymetallic species. In contrast, the Hg(II) complexes display well-defined structures with spectroscopic features characteristic for a HgS_2 and HgS_3 coordination mode at pH = 2.0 and 7.4, respectively. Stability data reflect a *ca.* 20 orders of magnitude larger affinity of the peptides for Hg(II) (log $\beta_{HgP}^{pH7.4} \approx 41$) than for Cu(I) (log $\beta_{CuP}^{pH7.4} \approx 18$). The different behaviour with the two metal ions demonstrates that the use of Hg(II) as a probe for Cu(I), coordinated by thiolate ligands in water, may not always be fully appropriate.

Significance to metallomics

Mercury(II) and copper(I) detoxification in cells involves similar sulphur-rich proteins, including metallothioneins. Short model peptides are used here to study the molecular interactions of these two soft cations with sequences containing three cysteine moieties found in these proteins. We demonstrate that the binding of Hg(II) and Cu(I) with these representative cysteine-rich sequences involves different molecular mechanisms, with the formation of various coordination complexes. Hence, the use of Hg(II) as a probe for Cu(I) coordination with sulphur-rich peptides or proteins in physiological conditions is demonstrated here to be not fully appropriate.

Introduction

Many metal ions, including Fe(II/III), Cu(I/II) or Zn(II), are essential micronutrients. Since both their deficiency and excess are harmful for the cells, the optimal concentration of these ions is controlled by regulation systems involving lots of proteins. Other metal ions, like Hg(II) and Cd(II), are toxic without any advantageous effects. The high affinity of these soft metal ions for soft sulphur bases, found in proteins and small ligands, such as glutathione, is one of the main factors leading to their toxicity. Indeed, interactions between these toxic metal ions and thiol-containing molecules induce misfolded protein structures or perturbation in the redox balance of the cells.

As a consequence of the similar coordination properties of the essential Cu(I) and the toxic Hg(II) ions, the cellular regulation and protection systems for controlling or reducing the concentration of these ions involve proteins with sulphur-rich metal coordination sites, usually dominated by Cys-thiolate donor groups. A varying number of Cys residues may allow the binding of Cu(I) or Hg(II) in isolated monometallic coordination sites or in polymetallic clusters. The strong preference of Hg(II) for a bis-thiolate coordination environment is reflected by the published structures of several elements of the bacterial mercury resistance system, MerP,[1] MerT,[2] the N-terminal domain of MerA[3] or the Hg(II)-bound form of the copper chaperone Atx1.[4] Nevertheless, there are also examples of structures with more Hg(II)–thiolate bonds, *e.g.* the distorted tetrahedral tetrathiolate Hg(II)-centre of rubredoxin,[5] or the tri- or tetra-coordinated metal ion environments in Hg(II)-bridged protein dimers, like those observed in the MerR metalloregulatory protein[6] or in the human

[a] INAC/SYMMES/Université Grenoble Alpes, CEA, CNRS, 38000 Grenoble, France. E-mail: pascale.delangle@cea.fr

[b] Department of Inorganic and Analytical Chemistry, University of Szeged, Dóm tér 7, Szeged H-6720, Hungary. E-mail: jancso@chem.u-szeged.hu

[c] BIG/LCBM/Université Grenoble Alpes, CEA, CNRS, (UMR 5249), 38000 Grenoble, France

copper chaperone HAH1.[7,8] Cu(I) can also accommodate a linear CuS$_2$-type coordination mode, as indicated by structural data on the copper efflux regulator CueR[9] or the metal binding domains of the copper transporter protein ATP7B.[10] Trigonal CuS$_3$ centres were proposed in the binuclear Cu(I)–thiolate core of the repressor protein CopY[11] and in one of the suggested metal-bridged dimeric forms of the copper chaperone CopZ,[12] whereas the Cu(I)-bridged HAH1 dimer[7] was shown also to include a fourth, weakly bound, thiolate in a pseudotetrahedral environment.

Di-, tri- or tetrathiolate coordination modes are also typical in polymetallic clusters. Metallothioneins (MTs) are small, cysteine-rich proteins, found in all kingdoms of life from prokaryotes to mammals. Several isoforms of MTs evolved with high diversity of amino acid sequences and, pursuant to this, with different metal ion preferences, 3D structures and proposed biological functions.[13,14] A novel approach for the classification of such a big family of proteins was developed by the groups of Capdevila and Atrian based on the metal binding features of MTs, *i.e.* on the criterion whether the MT binds Zn(II) either in homo or in heterometallic form, or only Cu(I) under physiological conditions.[15,16] Trigonally coordinated Cu(I) ions strongly dominate in Cu(I)-loaded MTs displaying also less abundant Cu(I)S$_2$ centres.[17,18] The only published Cu(I)-loaded MT crystal structure, a truncated form of the Cu(I)–MT of yeast, bears a Cu(I)$_8$S$_{10}$ core with six tri- and two di-coordinated metal ions where all Cys residues bridge two or three Cu(I) centres.[19] It was also suggested that a Cu(I)$_4$S$_6$ cluster could form in yeast MTs under low Cu(I) availability.[20] Indeed, the latter core contains only tri-coordinated Cu(I) and is widely used by nature in many other types of metalloproteins,[21] *e.g.* in the C-terminal domain of the membrane copper transporter Ctr1[22] or in various Cu(I)-activated transcription factors.[23,24] In contrast, Hg(II)–thiolate clusters in MTs were found to display a complicated mixture of di-, tri- and tetra-coordinated Hg(II) centres, with strong dependence on the applied conditions (pH, temperature, Hg(II) concentration, counter ions, *etc.*).[25,26]

An interesting strategy to better understand the individual contributions of specific short sequences to the overall affinity of proteins for metal ions is to design and study model peptides. This approach could eventually lead to the identification of relevant peptide-based motifs for heavy metal chelation. Some of the above described metal-binding sites have been probed by using oligopeptides encompassing the relevant metal binding sequences of the modelled proteins. The metal-binding features of the metalloregulator CueR and the metallochaperone Atx1, both encompassing 2 cysteines in their metal-binding domain, with different sequences between the Cys residues, were investigated *via* oligopeptide models of the relevant metal-binding loops.[27–33] A general finding was that the linear unstructured ligands, while displaying high affinity and interesting metal ion selectivity for Hg(II) or Cu(I) chelation, could not fully reproduce the efficiency of the modelled proteins.[28,31,33] Cyclisation of the linear Atx1 model, resulting in a more rigid skeleton with pre-oriented Cys-sidechains, was an important step forward leading to notably increased metal binding affinities.[27,28] The more challenging imitation of the HgS$_3$ type metal coordination sites

was successfully achieved by different approaches. Pecoraro *et al.* successfully applied single oligopeptide chain three-helix bundles[34] and three-stranded coiled coils[35] to settle three Cys residues into optimal position for accommodating the Hg(II) ion in a tri-coordinate fashion under slightly alkaline conditions. These tris-thiolate bound species were in a pH-dependent equilibrium with HgS$_2$ type complexes, characterized by apparent pK_a values ≥ 7.[34,35] Using a different strategy, tripodal pseudopeptide ligands were designed with cysteine or D-penicillamine (D-Pen) moieties grafted onto a nitrilotriacetic acid scaffold.[36,37] These constructs were able to stabilize the HgS$_3$ coordination mode in a broad pH-range, starting even at pH ∼ 5.5 with one of the D-Pen ligands.[36] Interestingly, the behaviour of the same ligands in binding Cu(I) was less straightforward. Depending on the bulkiness and hydrophobicity of the arms attached to the tripodal template, the formation of mononuclear and (Cu$_2$Lig)$_x$ type complexes with (Cu$_2$S$_3$)$_x$ cores was observed with high stabilities.[38,39] In a recently published article, the Hg(II) binding of the cyclic peptide **P^{3C}** incorporating a three Cys variant of the metal binding loop of Atx1 was discussed.[40] This cyclic solvent accessible peptide was considered as a predisposed structure that could pre-orient the Cys-sidechains for an easy accommodation of metal ions in a tri-coordinate fashion. The results confirmed the formation of a mononuclear Hg(II) complex with properties indicative of an HgS$_3$ coordination.

Peptide scaffolds similar to **P^{3C}** and comprising two typical metal binding motifs found in metallothioneins, namely the CxCxxC and CxCxC sequences,[41–43] are investigated in the present paper. Their binding properties for the two soft metal ions Cu(I) and Hg(II), exhibiting the largest affinities for metallothioneins, are studied and discussed in relation to their binding by detoxification systems.[26,44–46]

Experimental section

Materials

Materials and solvents were purchased from Sigma Aldrich, Fluka, Acros Organics and used without further purification. Amino acid building blocks, resins and coupling agents were purchased from NovaBiochem. For aqueous solutions, ultrapure laboratory grade MilliQ water was used (resistivity 18 MΩ cm).

Abbreviations

Ac$_2$O: acetic anhydride; AcN: acetonitrile; BCS: bathocuproinedisulfonate; DCM: dichloromethane; DIEA: *N*,*N*-diisopropylethylamine; DTNB: 5,5′-dithio-bis-(2-nitrobenzoic acid); EDT: ethanedithiol; Et$_2$O: diethyl ether; Fmoc: 9-fluorenylmethoxycarbonyl; HBTU: 2-(1*H*-benzotriazol-1-yl)-1,1,3,3-tetramethyluronium hexafluorophosphate; HOBt: hydroxybenzotriazole; MeOH: methanol; NMP: *N*-methyl-2-pyrrolidone; TFA: trifluoroacetic acid; TIS: triisopropylsilane.

Peptide synthesis and purification

Linear peptides. Ac-GCTCSCGSRP-NH$_2$ (**1^L**) and Ac-GTCSCGCSRP-NH$_2$ (**2^L**) peptides with acetyl and amide

protection at their two termini were synthesized by standard solid phase peptide synthesis following the Fmoc procedure. Rink Amide AM resin (200–400 mesh, 0.67 mmol g^{-1}) was used as solid support. The average coupling mixture consisted of 4 equiv. of protected amino acid building blocks, 4 equiv. of HOBt, 4 equiv. of HBTU and 8 equiv. of DIEA dissolved in NMP. The reaction time was 1 h. The noncomplete coupling was monitored by Kaiser's test.[47] To avoid the formation of deleted products, the acetylation of the unreacted amino groups was performed in a mixture of 10% Ac$_2$O and 10% DIEA in DCM after each coupling reaction. The Fmoc deprotection was achieved by 20% piperidine solution in NMP. The cleavage of the peptide from the resin and the removal of the sidechain protecting groups were performed in one step in the mixture of TFA/EDT/H$_2$O/phenol/TIS (92/2.5/2.5/2/1 V/V%) for 4 h. After evaporation, the residue was precipitated in ice cold Et$_2$O and centrifuged (6000 rpm, 15 min).

Cyclic peptides. For c(SRPGCTCSCG) (**1^C**), c(CSRPGTCSCG) (**2^C**) and c(CSRPGATCSCG) (**3^C**), linear precursors were first assembled on preloaded H-Gly-2-Cl-trityl resin (0.54 mmol g^{-1}) following the same method as described above. The protected precursor was cleaved from the resin by treatment with 2% TFA in DCM for 2 × 5 min. The solution was flushed into 20% pyridine in MeOH. After concentration, the residue was precipitated in ice cold Et$_2$O. The protected linear precursor (0.5 mM in DCM) was reacted with 3 equiv. of PyBOP and 4 equiv. of DIEA. After 2 h reaction time, the DCM was removed by evaporation and the residue was precipitated in ice cold Et$_2$O. The sidechain protecting groups were removed in TFA/EDT/H$_2$O/TIS (90/5/2.5/2.5 V/V%) for 2 h. After evaporation, the remaining solution was precipitated in ice cold Et$_2$O.

The crude products were purified by reversed phase HPLC on a Shimadzu LC-20 instrument equipped with a Phenomenex Synergi 4 µm fusion-RP 80 Å semi-preparative column. H$_2$O and acetonitrile with 0.1% TFA were used as eluents. The purity was checked by analytical HPLC and ESI-MS. Analytical RP-HPLC was performed using an analytical column (Chromolith® performance RP-18e 100-4.6 mm) at 1 mL min^{-1} flow rate (gradient 0–60% of AcN in 30 min). The synthesis of **P^{3C}** has been published earlier.[40] For the other peptides analytical HPLC and ESI-MS characterization is available in Table S1 and Fig. S1 in the ESI.†

Sample preparation for physicochemical studies

The cysteine residues of the peptides and Cu(I) are sensitive to oxidation; therefore all sample preparations and manipulations were performed in a glove box, under an argon atmosphere. Fresh solution was made for each experiment in the appropriate buffer. 10% acetonitrile in volume was added to the Cu(I) containing samples to overcome Cu(I) disproportion in water.[48] The final peptide concentration was determined by Ellman's procedure, where DTNB reacts with the free thiols forming TNB$^-$ (2-nitro-5-thiobenzoate) with ε^{412} = 14 150 M^{-1} cm^{-1}.[49,50] Cu(I) solution was made from Cu(CH$_3$CN)$_4$PF$_6$ salt in acetonitrile. The final concentration was determined by using BCS forming a stable Cu(BCS)$_2$ complex with ε^{483nm} = 13 300 M^{-1} cm^{-1}.[51]

A precise weight of high purity HgCl$_2$ was used to prepare Hg(II) stock solution in water (∼3 mM).

UV-Vis absorption and circular dichroism (CD) measurements

UV-Vis spectra were recorded on a Varian Cary 50 spectrophotometer equipped with optical fibers connected to an external cell holder in the glovebox. CD spectra were acquired with an Applied Photophysics Chirascan photometer. (1*S*)-(+)-10-Camphorsulfonic acid served as the calibration compound for the instrument. Spectra were recorded in the 320–190 nm wavelength range with 1 nm bandwidth and 2 s dwell time per point. For each sample 3 parallel spectra were recorded and the average of these spectra was smoothed by the Savitzky–Golay method with a "window size" 7. CD spectra are reported in molar ellipticity ([Θ] in units of deg cm^2 dmol^{-1}). [Θ] = θ_{obs}/(10lc), where θ_{obs} is the observed ellipticity in millidegrees, l is the optical path length in cm and c is the peptide concentration in mol dm^{-3}.

With Cu(I), titrations were performed in individually prepared samples because of the slow complex formation. 2.5 mL volumes of peptide solution (20–30 µM) in phosphate buffer (20 mM, pH = 7.4) were transferred into UV cells (1.0 cm path length) and then different (0.0–3.0) equivalents of Cu(I) were added to these samples. The samples were equilibrated for at least 2 hours. To ensure the thermodynamic equilibrium was reached, the absorbance was measured regularly. In the case of Hg(II) titrations, 2.5 mL of peptide solution (20–30 µM) in phosphate buffer (20 mM, pH = 7.4) was transferred into a UV cell (1.0 cm path length) and then aliquots of the Hg(II) ion solution (∼3 mM) were gradually added from 0.0 to 3.0 equivalents. pH titrations of the Hg(II) complexes were performed in pure water in the pH range of 2–11 by adding aliquots of 0.1 M KOH. The pH was measured using a Metrohm 702 SM Titrino equipped with a Mettler Toledo InLab® Micro electrode. pK_a values for the observed deprotonation processes were obtained by fitting the data by using the SPECFIT computer program.[52–55]

ESI-MS experiments

Mass spectra were acquired on a LXQ-linear ion trap (THERMO Scientific) instrument equipped with an electrospray ion source. Electrospray full scan spectra in the range of m/z = 50–2000 amu were obtained by infusion through a fused silica tubing at a flow rate of 2–10 µL min^{-1}. The solutions were analysed in negative and positive ion modes. The LXQ calibration (m/z = 50–2000) was achieved according to the standard calibration procedure from the manufacturer (mixture of caffeine, MRFA and Ultramark 1621). The temperature of the heated capillary for the LXQ was set in the range of 200–250 °C, the ion-spray voltage was in the range of 3–6 kV and the injection time was 5–200 ms. The ligand solution (100 µM) was prepared in ammonium acetate buffer (20 mM, pH = 6.9) and aliquots of the appropriate metal ion were then added.

Determination of apparent stabilities of the metal ion complexes

The apparent stability constants at a given pH were determined by UV-Vis titration in the presence of a competitor. The Cu(I)

complexes were prepared by adding 0.9 equivalents of Cu(I) to three samples of each peptide (50 μM) in phosphate buffer (20 mM, pH = 7.4)/acetonitrile (9/1 V/V). Then 4, 8 and 12 equivalents (with respect to Cu(I) concentration) of BCS were added, respectively. The samples were equilibrated until the absorbance stabilized. Stability constants were calculated considering the formation of the CuP mononuclear complexes at the beginning of the titration according to the following equation:

$$\beta_{11}^{\text{pH7.4}} = \frac{[\text{CuP}]}{[\text{Cu}][\text{P}]}$$

where CuP and P represent the complexed and free peptide at the pH of the studies, independent of the protonation state of the ligand, and Cu stands for the free Cu(I) ions.

The stabilities of the Hg(II)–peptide complex were determined at pH = 2.0 by using iodide (I⁻) as a competitor. Stability constants of the HgI$_n$ (n = 1–4) complexes were taken from the literature[56] and recalculated for the conditions of the experiments (pH = 2.0, I = 0.1 M NaClO₄) by applying the SIT model.[57,58] The molar absorption spectra of the four Hg(II)–I⁻ complexes were determined by titrating a Hg(II) solution by the continuous addition of aliquots of I⁻ solutions (0.01, 0.1 and 0.5 M KI). The recorded spectra were fitted with SPECFIT[52–55] by fixing the stability constants of the HgI$_n$ complexes. The peptide solutions were prepared in water (30 μM, I = 0.1 M NaClO₄) and the pH was adjusted by a 1.0 M HCl solution. Samples for the competition experiments were prepared by adding 1.0 equivalent of Hg(II) to the peptide solutions. They were then titrated by the I⁻ solutions by the same procedure and under the same conditions as described above. The pH of samples was under control throughout the experiments. SPECFIT[52–55] was used for the evaluation of spectra. The molar absorption spectra and the stabilities of the HgI$_n$ complexes were fixed in the fitting procedure, allowing one to calculate the apparent stability of the HgP binary and HgPI ternary complexes (see the equations below), as well as their molar absorption spectra.

$$\beta_{\text{HgP}}^{\text{pH2.0}} = \frac{[\text{HgP}]}{[\text{Hg}][\text{P}]}$$

$$\beta_{\text{HgPI}}^{\text{pH2.0}} = \frac{[\text{HgPI}]}{[\text{Hg}][\text{P}][\text{I}]}$$

In the equations above, HgP (or HgPI) and P represent the complexed and free peptide at the pH of the studies, independent of the protonation state of the ligand, and Hg and I stand for the free Hg(II) and I⁻ ions, respectively.

Determination of acid dissociation constants (pK_a)

Deprotonation processes of one of the linear peptide ligands, **1$^{\text{L}}$**, were followed by pH-potentiometric titrations in aqueous solution (T = 298.0 ± 0.1 K, c_{ligand} = 1.0 × 10⁻³ M, I = 0.1 M NaClO₄) following a protocol described earlier.[29] An automatic titration set, including a PC-controlled Dosimat 665 (Metrohm) autoburette and an Orion 710A precision digital pH-meter

equipped with an Orion 8103BNUWP Ross Ultra semi micro pH electrode, was used to carry out the experiments. Argon atmosphere in the titration cell was applied in order to prevent the oxidation of the ligand. The data obtained in two parallel titrations were fitted using the PSEQUAD computer program[59] based on the following general equilibrium process with the related equilibrium formation constants allowing the calculation of the pK_a values for the individual deprotonation steps:

$$q\text{H} + r\text{L} \rightleftharpoons \text{H}_q\text{L}_r$$
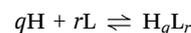
$$\beta_{\text{H}_q\text{L}_r} = \frac{[\text{H}_q\text{L}_r]}{[\text{H}]^q[\text{L}]^r}$$

where L denotes the non-protonated peptide and H the protons (charges are omitted for simplicity). Consequently, the composition of the neutral fully protonated peptide is H₃L. These pK_a values were used in the calculation of the thermodynamic stability constants for the HgL and HgHL complexes from the apparent stabilities obtained at pH = 2.0. Details of these calculations are found in the ESI.† Note that 'L' for the ligands is used in the text where the actual protonation states of the ligands/complexes are taken into account in calculations or in the description of species, whereas 'P' denotes the peptides in general, independent of their protonation states, as in the calculation of the apparent stabilities.

Modelling of the trithiolate mercury complexes

The six peptides were modelled in the apo and Hg(II)-bound form with a HgS₃ trigonal coordination. In the absence of structures for all the peptides but **P$^{\text{3C}}$**, initial coordinates were built with the CHARMM program[60] from standard values for the internal bonds, angles and dihedrals of amino acids in proteins. For peptide **P$^{\text{3C}}$**, initial coordinates were either generated as for other peptides or taken from the solution NMR structure of the Hg**P$^{\text{3C}}$** complex.[40]

Model parameters. For the holo peptides, a bonded model of the mercury site was used. Molecular mechanics force field parameters around mercury, absent from the CHARMM force fields, were deduced from *ab initio* DFT/B3LYP[61–63] calculations on the model system Hg²⁺–(S–CH₂–CH₃)₃⁻ of tri-coordinated mercury using the Gaussian program.[64] A total charge of −1 in the singlet spin state and using the LanL2dz basis set was used. Bonded parameters were obtained by harmonic potential fitting of *ab initio* scans of the Hg–S distance, C–S–Hg angle and Hg–S–S–S improper angle. In this trigonal model, the S–Hg distance is 2.794 Å, the Cβ–S–Hg angle is 125° and the Hg–S–S–S improper angle (calculated with Hg above the 3 sulfur atom plane in the counter clockwise direction) is 7.8°. Charges were obtained from RESP calculations following DFT/B3LYP optimization. Calculated charges are: Hg: +0.968, S: −0.798, all C(bonded to 2 hydrogens): 0.173, all C(bonded to 3 hydrogens): 0.069. van der Waals parameters were taken from the work of Šebesta *et al.*[65] for Hg: ε = 1.955 kcal mol⁻¹; R = 2.8 Å.

Molecular dynamics simulations. The geometries of the peptides were relaxed in vacuum by 1000-step energy minimization using the conjugated gradient method until the root-mean-square

(RMS) energy gradient was lower than 0.1 kcal mol^{-1} Å^{-1}. Then the peptides were simulated in implicit water using the implicit solvent method EEF1 and the adapted extended atom CHARMM19_EEF1 force field.[66] The systems were subjected to 40 to 300 ns MD simulations (depending on the convergence speed) using Langevin dynamics with a time step of 2 fs and a damping factor f_β of 20 ps^{-1} applied on non-hydrogen atoms. All peptides were simulated in the apo (no Hg) and holo (with Hg bound) forms.

Results and discussion

Peptide design and synthesis

The cyclic peptide $\mathbf{P^{3C}}$ with three cysteine sidechains preoriented for Hg(II) coordination was recently reported by our group.[40] All spectroscopic data obtained for the Hg$\mathbf{P^{3C}}$ mononuclear complex point to a HgS$_3$ coordination mode, which is stable over a large pH range (pH = 5–9).

Five new peptides (Scheme 1) were designed in this work to monitor the effects of introducing a CxCxC motif instead of the CxCxxC sequence found in $\mathbf{P^{3C}}$ on the Cu(I) and Hg(II) complexation features. The positions of the three cysteines in the sequence of the newly designed linear and cyclic peptides were varied. An xPGx β turn inducing motif was introduced in the sequences of the cyclic peptides to rigidify the scaffold containing the metal-binding fragment CxCxC next to the turn in $\mathbf{1^C}$ or one amino acid apart in $\mathbf{2^C}$.[28,67–69] $\mathbf{1^L}$ and $\mathbf{2^L}$ linear analogues of the cyclic decapeptides $\mathbf{1^C}$ and $\mathbf{2^C}$ were synthesized to determine the impact of the cyclisation and flexibility of the backbone on the coordination properties. Finally, an additional amino acid, namely alanine, was inserted in peptide $\mathbf{3^C}$ with the idea of promoting larger flexibility in the cysteine sidechain orientation.

Cu(I) complexes

One of the six investigated peptides, $\mathbf{P^{3C}}$, was previously demonstrated to stabilize the HgS$_3$ coordination in a mononuclear complex.[40] This raised the question whether a CuS$_3$ geometry could also be observed with the latter peptide and with the new 3-Cys containing peptides presented in this paper. Cu(I) complexation of the ligands was studied by UV-Vis and CD spectroscopy and ESI-MS. All the six peptides display a rather similar behaviour; therefore studies with peptide $\mathbf{1^C}$ are presented here to illustrate the Cu(I)-binding features of the whole series. The titration of the peptides with Cu(I) at pH 7.4 was followed
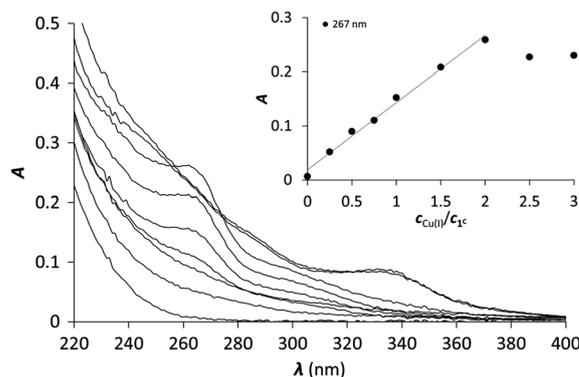

Fig. 1 UV spectra of $\mathbf{1^C}$ titrated with Cu(I) (equilibration time = 2 hours). The inset shows the increase of the absorbance at 263 nm as a function of $c_{Cu(I)}/c_{peptide}$ ratio ($c_{peptide}$ = 30 µM in phosphate buffer, 20 mM, pH = 7.4).

by UV-Vis spectroscopy. The absorbance stabilizes surprisingly slowly with the equilibrium reached only after *ca.* 2 hours. Such long equilibration times were not observed before in similar systems with thiolate containing peptides or pseudopeptides, even when Cu(I) clusters were formed from the very beginning of the titration.[28,38,39] Titrations using individual samples were therefore conducted with Cu(I) to peptide concentration ratios from 0.0 to 3.0 in 0.25–0.5 steps to allow for long equilibration times and ensure that the thermodynamic equilibrium is reached. Fig. 1 shows the results of the UV titration of peptide $\mathbf{1^C}$ with Cu(I) at equilibrium. An intense band, characteristic for the S$^-$ to Cu(I) charge transfer transition (LMCT),[70] emerges at λ = 263 nm with increasing Cu(I) concentration. The absorbance increases linearly up to 2.0 equiv. of Cu(I). The breakpoint observed for 2 equiv. of Cu(I) per peptide is indicative of the formation of polymetallic species with (Cu$_2$P)$_n$ overall stoichiometry as previously observed with 3-Cys-containing tripodal peptide-like ligands.[38,39] As seen before, the intensity of the S$^-$ to Cu(I) LMCT is not sensitive to the composition of the complex and provides information only about the number of Cu(I)–thiolate bonds.[38,39,71,72] The extinction coefficients ε = 6000–7000 M^{-1} cm^{-1} per bound Cu(I) reported in Table 1 are in good agreement with data reported with other thiolate–Cu(I) complexes.[71,73]

Cu(I) complex formation was also followed by recording CD spectra of the individually prepared samples. As a result of Cu(I) additions, the spectra significantly change compared to the free ligand and signals appear in the S$^-$ to Cu(I) LMCT region (260–320 nm). However, the molar ellipticities are
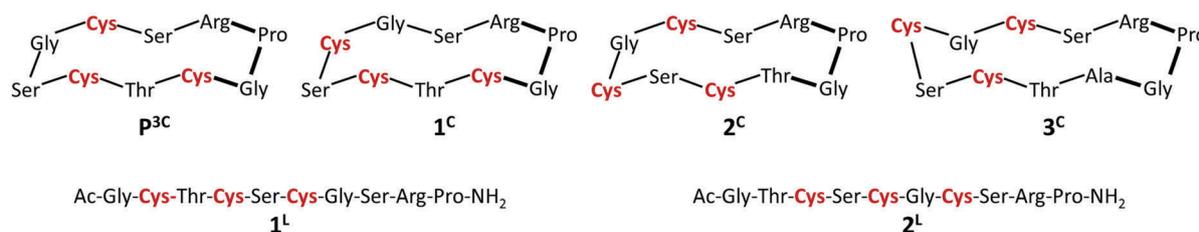
Scheme 1 Sequences of the studied peptides. Bonds in the turn motif are indicated in bold and the coordinating cysteine residues are highlighted in red.

Table 1 LMCT band characteristics for Cu(ɪ) and Hg(ɪɪ) complexes of the studied peptides

	CuP		HgP	
	λ (nm)	ε (M^{-1} cm^{-1})	λ (nm)	ε (M^{-1} cm^{-1})
P^{3C}	259	7500	240	17 500[40]
			270	10 200
1^C	267	6700	240	13 800
			280	7300
1^L	267	6100	240	14 900
			280	9400
2^C	267	6200	240	15 000
			280	7700
2^L	262	6500	240	14 600
			280	7700
3^C	261	6400	240	14 500
			280	7800

Table 2 Apparent stability constants, deprotonation constants and some estimated stability data (all in the form of their logarithms) of the Hg(ɪɪ) and Cu(ɪ) complexes. For the experimentally determined values errors on the last characters are indicated in parentheses

	log $\beta_{CuP}^{pH7.4\ a}$	log $\beta_{HgP}^{pH2.0}$	log $\beta_{HgP}^{pH7.4\ b}$	p$K_{HgHL}^{HgL\ c}$	log β_{HgHL}^{b}	log β_{HgL}^{b}
P^{3C}	18.1(1)	27.2(1)	40.9	4.3(1)[40]	48.7	44.4
1^C	17.3(3)	27.3(1)	40.5	4.8(1)	48.8	44.0
1^L	17.4(2)	27.1(1)	40.0	5.1(1)	48.6	43.5
2^C	17.8(4)	27.2(1)	40.7	4.5(1)	48.7	44.2
2^L	17.8(2)	27.0(1)	40.0	5.0(1)	48.5	43.5
3^C	17.9(4)	27.5(1)	41.0	4.5(1)	49.0	44.5

^{a} The apparent stabilities were calculated by assuming the presence of only mononuclear complexes. ^{b} Apparent stability constants for pH 7.4 and formation constants of the HgHL and HgL species were estimated from the apparent stabilities obtained at pH = 2.0, as described in the ESI. ^{c} The pK values characterize the HgHL $\rightleftharpoons$ HgL + H$^+$ process.

relatively low ($[\Theta] < 1 \times 10^4$ deg cm^2 dmol^{-1}) compared to those obtained with other species involving 3 coordinated Cys ($[\Theta] = 4 \times 10^4 - 8 \times 10^4$ deg cm^2 dmol^{-1}).[38,39,71] Moreover, no clear tendency can be observed in the evolution of the spectra upon Cu(ɪ) addition up to 2.0 equivalents, as shown in Fig. S2 (ESI†). The mostly affected region falls below 250 nm, where the negative CD band is attributed to $\pi \rightarrow \pi^\star$ and possibly overlapping n $\rightarrow \pi^\star$ transitions, both belonging to the amide bonds of the peptide backbone,[74,75] which suggests a conformational rearrangement upon Cu(ɪ) addition. Since CD spectroscopy is more sensitive to the structure around Cu(ɪ) than UV, these results indicate that the free peptides transform into more than one Cu(ɪ) species. This assumption is confirmed by ESI-MS measurements in ammonium acetate buffer at pH 6.9 (Fig. S3, ESI†). Spectra recorded for samples with the peptides and 0.9 equivalents of Cu(ɪ) show the formation of mononuclear complexes, CuP, and several polynuclear species, like Cu$_4$P$_2$ and Cu$_4$P$_3$. With the increase of the Cu(ɪ) concentration, further species of higher nuclearity (Cu$_8$P$_4$, Cu$_7$P$_3$, Cu$_9$P$_3$) are detected. Therefore, the CD and ESI-MS experiments demonstrate that the apparently simple evolution of the LMCT bands in the UV titration is in fact due to the formation of a mixture of many polynuclear thiolate complexes.

Copper binding affinities were determined in the presence of BCS as a competitor. BCS forms a well-characterised Cu(BCS)$_2$ complex with Cu(ɪ) according to eqn (1).

$$Cu^+ + 2BCS^{2-} \rightleftharpoons [Cu(BCS)_2]^{3-} \quad \log \beta = 19.8 \quad (1)$$
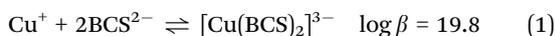
This complex has an intense orange colour and a maximal absorbance at λ = 483 nm with an extinction coefficient ε = 13 300 M^{-1} cm^{-1}.[51] Solutions of the Cu(ɪ)–peptide complexes (Cu(ɪ) : P ratio = 0.9 : 1) were titrated with BCS and the amount of Cu(ɪ) displaced from the peptide by BCS was quantified based on the known absorption of the Cu(BCS)$_2$ complex. Since several Cu(ɪ) complexes are formed with the six peptides, the fit of the spectroscopic competition results could not be perfectly implemented with a given complex stoichiometry. Hence, the apparent stability constants were calculated considering the formation of a CuP complex. The log $\beta_{CuP}^{pH7.4}$ values are presented in Table 2.

All peptides display high affinity towards Cu(ɪ) in the range typical of Cu(ɪ) chaperone proteins, like Atx1.[22]

Hence, Cu(ɪ) binding to the investigated 3-Cys containing peptides is characterized by a rather complicated speciation at pH = 7.4. Indeed, although the UV profile appears simple with a single endpoint at 2 equivalents of Cu(ɪ), ESI-MS and CD clearly evidence several clusters, even with low Cu(ɪ) concentration. This complicated mixture of species observed for the whole series of peptides highly contrasts with previous results obtained with tripodal pseudopeptides also incorporating three cysteine moieties, which form Cu(ɪ) complexes, resembling those formed in metallothioneins.[39,71,76] Indeed, the preorientation of the three thiolate groups in the tripodal pseudopeptides induces a well-defined metal binding cavity, stabilized by a network of hydrogen bonds.[39] This structure perfectly controls the speciation of the Cu(ɪ) complexes with only two identified species, namely the mononuclear complex and the cluster Cu$_6$S$_9$ both with Cu(ɪ) ions in trithiolate environments.[39,76] More recently, the highly constrained tetrapeptide Ac-Cys-ᴅ-Pro-Pro-Cys-NH$_2$ with a strong turn was shown to form exclusively a Cu$_4$S$_6$ core.[77] The larger flexibility of the peptides described here could be responsible for the lack of control of the speciation of the Cu(ɪ) complexes and ultimately for the formation of a mixture of polymetallic species, with quite large stability. The determined apparent stability constants are similar in the whole peptide series, within the range of experimental errors, indicating that the structural differences have only a minor effect, if any, on the stability of the Cu(ɪ) complexes.

Hg(ɪɪ) complexes

Hg(ɪɪ) is a metal ion with soft character according to Pearson's theory,[78] and as such, an often used probe of the oxygen and water sensitive Cu(ɪ). The cyclic peptide **P^{3C}** has been recently demonstrated to form a complex with Hg(ɪɪ) in a HgS$_3$ coordination environment, which is stable over a large pH range. Besides, the protonation of the mononuclear complex Hg**P^{3C}** happens at a relatively low pH (pK_a value of 4.3) to produce a species with HgS$_2$ geometry.[40] Hg(ɪɪ) binding of the new series of peptides was therefore studied to reveal whether the behaviour of **P^{3C}** with Hg(ɪɪ) is specific to the structure of this cyclic

peptide or common for peptide sequences encompassing three Cys residues in a CxCxxC or CxCxC arrangement.

Hg(II) binding at physiological pH. The S^- to Hg(II) LMCT bands of mercury–thiolate complexes are indicative of the metal ion coordination number and geometry, in contrast to similar bands of Cu(I)–thiolates. The HgS_3 coordination mode is characterized by an LMCT band in the wavelength range of 240–320 nm,[37,79] while the di-coordinate HgS_2 structures leave their fingerprint only in the higher energy UV region.[28,80,81] Accordingly, the Hg(II) binding properties of the peptides were studied by UV-Vis spectroscopy at pH = 7.4. Titrations were conducted by gradually adding 0.1 equivalent of Hg(II) to the peptide solutions. The absorbance values stabilized after Hg(II) additions much faster (in less than 5 minutes) compared to the complexation of Cu(I) by the same peptides, which might be a result of a simpler speciation in the Hg(II)–ligand systems. All peptides showed very similar behaviour to P^{3C}.[40] The UV titration of 1^C is presented in Fig. 2 as an example. With the increase of metal ion concentration, two intense bands emerge at $\lambda \sim 240$ and 280 nm with molar absorption coefficients (Table 1) similar to those previously reported for HgS_3 type complexes.[36,37,80] Absorbances increase linearly up to 1:1 Hg(II)–peptide ratios, which reflects the formation of a single mononuclear complex, where Hg(II) is very likely coordinated by the three cysteine thiolates of the peptides. In the presence of Hg(II) in excess, a decrease of the absorbances at the selected wavelength values can be observed, indicating that the mononuclear complex transforms into polymetallic species with Hg(II) ions coordinated by only two cysteine thiolate residues.[28,80,81] Besides, the second endpoint observed at 1.5 equiv. of Hg(II) strongly suggests the formation of Hg_3P_2 complexes.

ESI-MS experiments performed in ammonium acetate buffer at pH 6.9 support well the UV spectroscopic results (Fig. 3). The spectrum of 1^C with 1.0 equivalent of Hg(II) clearly shows the presence of the mononuclear HgP complex in the forms of a $[Hg1^C]^{2+}$ and a $[Hg1^C–H]^+$ ion with $m/z = 576.8$ and 1152.3, respectively. The spectrum recorded with 1.5 equivalents of Hg(II) indicates the formation of new species. The major detected complex is Hg_3P_2 in the forms of $[Hg_3(1^C)_2–4H + Na]^{3+}$

and $[Hg_3(1^C)_2–4H]^{2+}$ with $m/z = 841.7$ and 1250.8, respectively. This species is compatible with the HgS_2 coordination environment of the metal ions. When 2.0 equivalents of Hg(II) are added, Hg_3P_2 and Hg_2P ($[Hg_2(1^C)–2H]^{2+}$; $m/z = 675.8$) can be detected in similar amounts. This mixture of complexes may explain the slight increase of the absorbance above 1.5 equivalents of Hg(II) per peptide.

All the peptides showed the formation of Hg(II) complexes with a simple speciation as described recently with the P^{3C} cyclic decapeptide.[40] The mononuclear complexes with features characterizing a trithiolate coordination are formed at physiological pH, as also extensively reported for the Hg(II) complexes of triple coiled-coil peptides.[34,35] Contrary to the latter systems, which define a highly protected hydrophobic metal-binding pocket, the flexible structure of the cyclic and linear peptides makes the transformation of the trithiolate coordination into the preferred dithiolate coordination possible in excess of Hg(II) in Hg_3P_2 complexes.

Protonation of the HgL complex. The absorbance at 280 nm, characteristic of the HgS_3 geometry in the Hg(II) peptide complexes, decreases significantly with decreasing pH, which indicates the protonation of one cysteine to afford a linear HgS_2 complex at low pH, as observed previously with P^{3C}.[40] Fig. 4 shows the pH titration for $Hg1^C$ as an example. The spectroscopic data were satisfactorily fitted with one pK_a value according to the following equation:

$$HgHL \rightleftharpoons HgL + H \quad K_{HgHL}^{HgL} = \frac{[HgL][H]}{[HgHL]} \quad (2)$$

where [HgHL] and [HgL] denote the equilibrium concentrations of the mononuclear complexes including the peptide in different protonation states.

Fig. 3 (+)ESI-MS spectra registered for 1^C with different equivalents of Hg(II) in ammonium acetate buffer (20 mM, pH = 6.9). The comparison of the experimental and calculated isotopic envelop of the detected species is also presented. Asterisks mark the sodium adduct of the corresponding species. The notation 1^C refers here to the neutral free peptide.
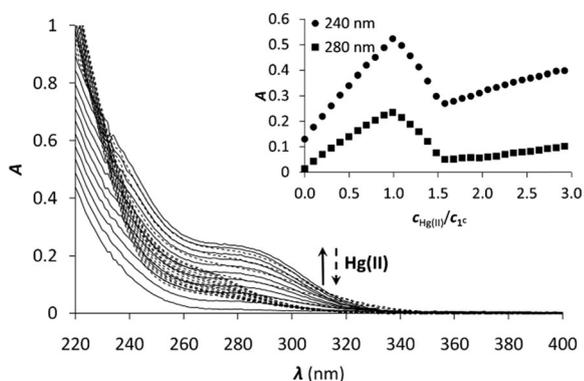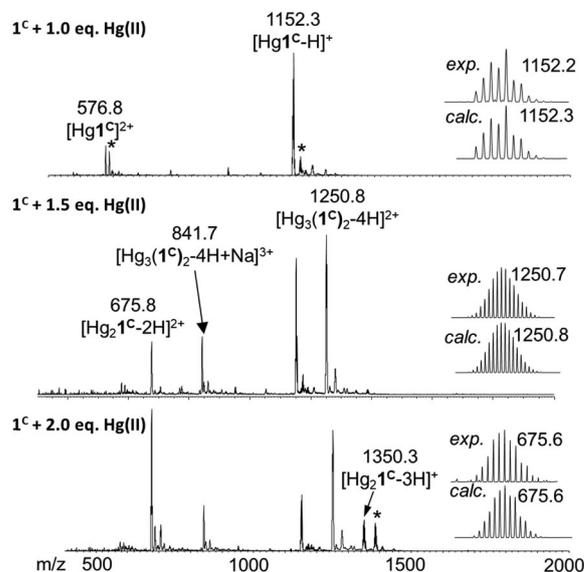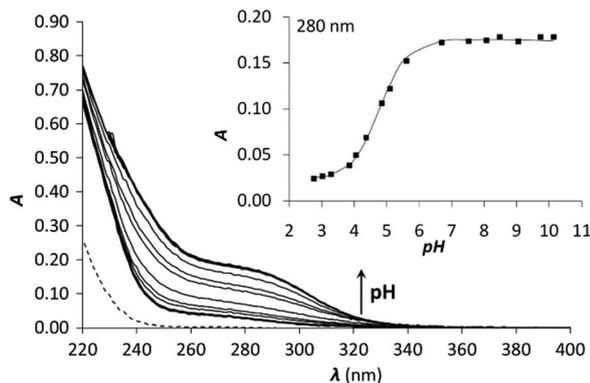

Fig. 2 UV titration of 1^C with Hg(II) in phosphate buffer (20 mM, pH = 7.4). The inset shows the increase of the absorbance at 240 and 280 nm as a function of $c_{Hg(II)}/c_{peptide}$ ratio ($c_{peptide} = 30\ \mu M$).

Fig. 4 pH titration of **1^C** with 1.0 equivalent of Hg(II). The dashed line represents the spectrum of free **1^C** at pH = 2. The inset shows the evolution of the absorbance as a function of pH at 280 nm. Symbols represent the experimental points and the line is the fitted absorbance obtained by SPECFIT.

The pK_a of the Hg(II)–peptide complexes (see Table 2) follow the order of **P^{3C}** < **3^C** ≈ **2^C** < **1^C** < **2^L** ≈ **1^L**. However, the differences observed between the pK_a values in the series of peptides (maximum difference = 0.8) are quite small, which reflects the weak influence of the pattern of the three Cys residues (CxCxC or CxCxxC) and the separation of the metal binding fragment from the turn motif. **P^{3C}** incorporating the CxCxxC sequence forms the HgS$_3$ coordination mode at a slightly lower pH than the other cyclic peptides. A larger separation from the PG-turn also seems to be favourable for the formation of the tris-thiolate complex in **3^C**. The highest pK_a values are seen for the two linear peptides, which may be a consequence of their larger flexibility and a more significant reorganization necessary for the coordination of the third Cys sidechain. It is rather interesting that even the latter data (Table 2) are 1.7–1.8 log units lower than the pK_a observed for the Hg(II)-complex of the tris-cysteine functionalized tripodal pseudopeptide ligand with amidated carboxyl groups,[37] or of the three-stranded coiled coils (pK_a values of 8.6 and 7.6 for sites d and a, respectively).[34] This might be related to the presumably very different water-accessibility of the thiol groups, as hinted recently.[40]

Stabilities of the Hg(II) complexes. Due to the high thiophilicity of Hg(II), the determination of the stability of the complexes is rather challenging. Competition titrations with iodide ions were performed to measure the apparent stability constants at pH = 2.0. To the best of our knowledge, this is the first time that the well-characterized Hg(II)-complexing ability of iodide has been utilized for the determination of the stability of Hg(II)–thiolate complexes, which is probably due to the presence of several iodo complexes. According to the observed pH-dependent transformation of the Hg(II)–peptide complexes, the apparent stabilities determined at pH = 2.0 mostly correspond to the species with a HgS$_2$ structure. Hg(II) has been shown to form iodo complexes in four consecutive steps characterized by large formation constants.[56] In spite of these large iodo complex stabilities, a high concentration of I$^-$ (1500–2000 equiv.) was

necessary to withdraw Hg(II) from the peptide complexes which required the use of a background electrolyte (I = 0.1 M NaClO$_4$) to lessen the change in the ionic strength during the titrations.

Therefore, the published stabilities of the iodo complexes were recalculated by applying the SIT model to the conditions of the experiments,[57,58] leading to the following formation constants: $\log \beta_{[HgI]^+}$ = 13.05, $\log \beta_{[HgI_2]}$ = 24.09, $\log \beta_{[HgI_3]^-}$ = 27.84, $\log \beta_{[HgI_4]_2^-}$ = 29.91. The result of the titration of Hg(II) with KI and the obtained molar spectra of the forming Hg(II)–I$^-$ complexes can be seen in Fig. 5A and Fig. S4 (ESI†), respectively.

Samples of the peptides containing 1.0 equivalent of Hg(II) were titrated with I$^-$ and the recorded spectra are presented in Fig. 5B. The first phase of the titrations, *i.e.* up to the presence of 10 equivalents of I$^-$, does not reflect considerable changes in the recorded spectra. Further addition of I$^-$ ions results in the appearance of new bands characteristic for the [HgI$_3$]$^-$ and [HgI$_4$]$^{2-}$ species (compare to the spectra in Fig. S4, ESI†). A complete displacement of Hg(II) from the peptide complexes is achieved at *ca.* 2000 equiv. of I$^-$.

The obtained spectra were fitted by SPECFIT by fixing the $\log \beta$ values and the molar spectra of the Hg(II)–I$^-$ complexes. The best fits were obtained when the formation of a mixed ligand complex, HgPI, was also included in the models, besides the HgP species (inset in Fig. 5B). The appearance of such species is probably a consequence of the flexibility of the peptide structures. The HgPI complexes are present only in
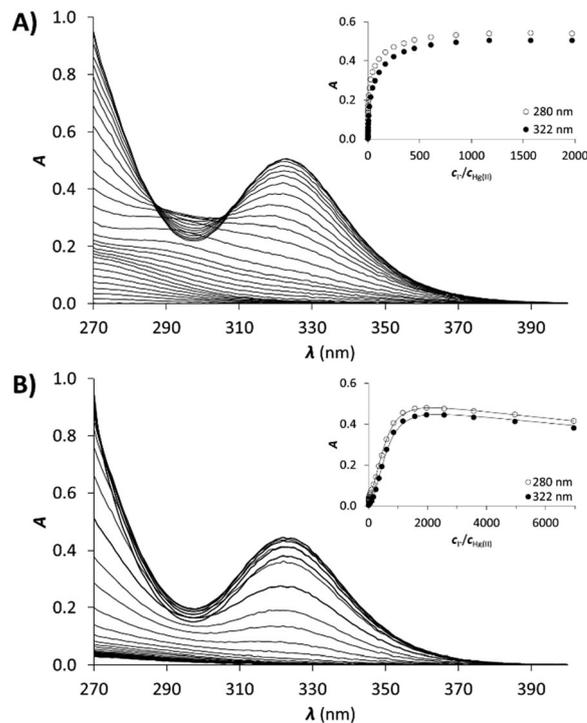

Fig. 5 UV spectra recorded in the titration of (A) Hg(II) and (B) Hg**1^C** with I$^-$. pH = 2.0, $c_{Hg(II)}$ = 30 μM (A), $c_{Hg(II)}$ = $c_{peptide}$ = 30 μM (B). The insets show the evolution of the absorbance at 322 nm (●) and 280 nm (○). Symbols represent the experimental data, and solid lines represent the absorbances calculated by SPECFIT.

the beginning part of the titrations in a *ca.* 20% relative proportion, except for Hg**P**[3C] where a somewhat larger fraction of HgPI could be observed. The formation of the mixed ligand complexes, according to the HgP + I $\rightleftharpoons$ HgPI equation, is characterized by stabilities falling in the range of $\log K \sim$ 1.5–2.5. The apparent stability constants determined for the HgP complexes (Table 2) indicate rather similar affinities of Hg(II) to all peptides. Considering that at pH = 2.0 Hg(II) is coordinated only by two thiolate units, it is a plausible assumption that the preorientation of the donor groups has only a modest influence on the stabilities and the high thiophilicity of Hg(II) easily governs the formation of the favoured HgS_2 structures. Formation constants for the different forms of the HgP species, *i.e.* for HgHL and HgL (where L denotes the fully deprotonated peptide), and apparent stabilities for pH = 7.4, were also estimated from the relevant conditional stability constants ($\log \beta_{HgP}^{pH2.0}$) by applying the pK_a values of the HgHL $\rightleftharpoons$ HgL + H processes (Table 2) and the pK_a values obtained for one of the free ligands, pK_a^{HL} = 9.26(1); p$K_a^{H_2L}$ = 8.56(1); p$K_a^{H_3L}$ = 7.67(1) (see the Experimental part and the ESI†). The stability constants estimated for the Hg(II)–trithiolate HgL complexes span over a small range (maximum difference, $\Delta\log\beta_{HgP}$ = 1) demonstrating a weak influence of the Cys-sidechain orientations in the chosen sequences (Table 2). Nevertheless, the two linear peptides display a slightly weaker affinity suggesting the need for a more pronounced rearrangement of the Cys sidechains. It is noteworthy to compare these data to the stability constants of Hg(II)–bisthiolate complexes of highly constrained bis-thiol ligands. Our peptides, indeed, display very similar Hg(II)-binding affinities to that of the well-known soft metal ion chelator 2,3-dimercaptopropan-1-ol (BAL) ($\log\beta_{HgL}$ = 44.8),[82] which forms a highly stable 5-membered chelate ring around the metal ion. Comparison of our data to the stability of the HgL species of the tetrapeptide C$_D$PPC ($\log\beta_{HgL}$ = 40.0)[81] clearly indicates that the structure of our peptides is prone to easily rearrange to a suitable form for the tridentate coordination of Hg(II) and thus the larger number of Hg(II)–thiolate bonds is revealed by higher affinities.

Modelling of the trithiolate HgL complexes

The six peptides were modelled in the apo and Hg(II)-bound form with a HgS_3 trigonal coordination (see Experimental section for methods). Several independent simulations were run: first, for the Hg(II)-bound peptides three different simulations were run varying the orders of the cysteine sulfur atoms defining the Hg–S–S improper angle; then, for each best energy conformation in each system, new simulations for the related systems were run starting from there. The energy values reported in Table S2 (ESI†) refer to the simulation leading to the minimum average total energy for each peptide (over all simulations). Binding of Hg(II) to linear or cyclic peptides always results in stabilization meaning that the peptide structure organizes the 3 cysteine residues in an environment appropriate for HgS_3 coordination. The stabilization expressed as $\Delta E = E(HgP) - E(P)$ is remarkably similar for all four cyclic peptides (between −11 and −12.8 kcal mol^{-1} from Table S2, ESI†)
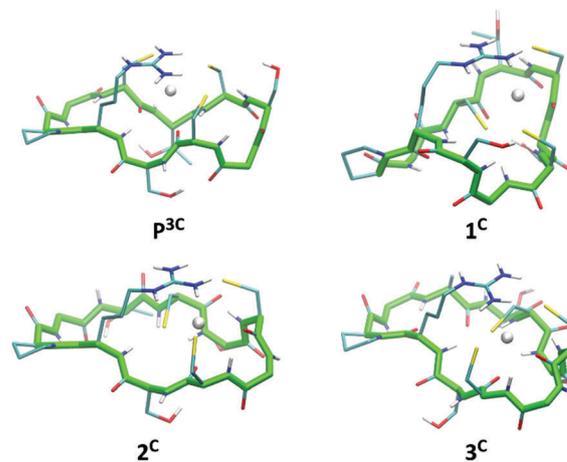

Fig. 6 Energy minimized structures of the 4 cyclic peptides in their Hg(II)-bound form (oriented with respect to the position of backbone atom coordinates of residues 1 to 10).

with a relative error ($\Delta E/E$) less than 1%. This stabilization varies from −13.1 to −9.5 kcal mol^{-1} for the two linear peptides; however, this slightly larger difference may be due to an incomplete conformational search of the highly flexible linear apo peptides. Hence, the calculated stabilization energies, ΔE, are very similar in the series of peptides, which is in agreement with the comparable values of the stability constants of the HgL complexes determined experimentally (Table 2). Models of energy minimized structures of the Hg(II)-bound peptides, starting from the frame with the lowest potential energy during the dynamics simulation leading to minimum average total energy, are shown in Fig. 6 and Fig. S5 (ESI†) for cyclic and linear peptides, respectively. The three cysteine binding chains are well-disposed to afford the trithiolate coordination of the mercury ion in the six structures. In all the complexes, the positively charged sidechain of arginine (charge +1) is capping the HgS_3, negatively charged binding site (charge −1), providing stabilizing electrostatic interactions.

Conclusions

Model peptides containing cysteine-rich sequences found in metallothioneins were studied for their metal-binding properties in relation to metal detoxification mechanisms. The two soft ions Cu(I) and Hg(II) were selected since they exhibit the largest affinities for these small detoxification proteins among endogenous and toxic metal ions, respectively. Three cysteine residues were introduced in CxCxxC and CxCxC motifs in different positions within the sequence, in linear and cyclic derivatives. Overall, the six peptides display rather similar behaviour, which evidences minor contributions of the position of the three cysteine residues or cyclisation to the formation and stability of the Hg(II) and Cu(I) complexes.

Cu(I) binding to the series of peptides at physiological pH revealed to be rather complicated, with the formation of a mixture of polymetallic species. In contrast, cysteine-rich highly structured peptides[77] or peptide-like ligands[39,76] are able to

control the formation of well-defined Cu(I) complexes. Consequently, the complicated Cu(I)-complex speciation of the series of peptides, reported in this paper, has been assigned to their significantly larger flexibility. However, despite the formation of many polymetallic species, large affinity is achieved for the soft Cu(I) cation at physiological pH (10^{17}–10^{18}).

The binding of Hg(II), another soft metal ion often used as a probe for the oxygen and water sensitive Cu(I), demonstrates that the complexity of the Cu(I) speciation is due to the peculiar behaviour of Cu(I)–thiolate complexes in water and not to the cysteine-rich sequences chosen for the peptides. Interestingly, the HgS$_3$ coordination mode is stable over a large pH-range for all studied peptide complexes. Indeed, the protonation of the complex to give the HgS$_2$ linear coordination is observed with pK_a values ranging from 4.3 to 5.1, making the trithiolate coordination the major binding mode at physiological pH whatever the peptide sequence. The stabilities of the Hg(II) complexes (10^{40}–10^{41} at pH 7.4) are of the same order of magnitude as those reported for high affinity sulphur chelating agents such as BAL.[82] The large stability constants together with the low pK_a values and simulated structures clearly indicate that all the peptide sequences studied in this paper are adapted for an efficient trithiolate coordination of the thiophilic cation Hg(II).

Importantly, the striking differences observed in the coordination of Hg(II) and Cu(I) with the series of peptides indicate different molecular mechanisms involved in their binding to detoxification proteins. The sulphur-rich peptides studied here show more than 20 orders of magnitude larger affinity at pH 7.4 for Hg(II) ($\log \beta_{HgP}^{pH7.4} \approx 41$) than for Cu(I) ($\log \beta_{CuP}^{pH7.4} \approx 18$), due to the significantly softer character of Hg(II). Most importantly, Hg(II) forms well-defined complexes, whereas Cu(I)-coordination leads to mixtures of polymetallic species. This demonstrates the peculiar behaviour of Cu(I) thiolate complexes in water. Only highly constrained peptide sequences are able to promote the formation of well-defined Cu(I) complexes. The peptides studied here are probably too flexible to achieve such a control for Cu(I). Hence, the use of Hg(II) as a probe for Cu(I) coordination with sulphur-rich peptides or proteins in physiological conditions is demonstrated here to be not fully appropriate.

Conflicts of interest

There are no conflicts to declare.

Acknowledgements

References

1 R. A. Steele and S. J. Opella, Structures of the Reduced and Mercury-Bound Forms of MerP, the Periplasmic Protein from the Bacterial Mercury Detoxification System, *Biochemistry*, 1997, **36**, 6885–6895.

2 E. Rossy, O. Sénèque, D. Lascoux, D. Lemaire, S. Crouzy, P. Delangle and J. Covès, Is the cytoplasmic loop of MerT, the mercuric ion transport protein, involved in mercury transfer to the mercuric reductase?, *FEBS Lett.*, 2004, **575**, 86–90.

3 R. Ledwidge, B. Patel, A. Dong, D. Fiedler, M. Falkowski, J. Zelikova, A. O. Summers, E. F. Pai and S. M. Miller, NmerA, the Metal Binding Domain of Mercuric Ion Reductase, Removes Hg^{2+} from Proteins, Delivers It to the Catalytic Core, and Protects Cells under Glutathione-Depleted Conditions, *Biochemistry*, 2005, **44**, 11402–11416.

4 A. C. Rosenzweig, D. L. Huffman, M. Y. Hou, A. K. Wernimont, R. A. Pufahl and T. V. O'Halloran, Crystal structure of the Atx1 metallochaperone protein at 1.02 Å resolution, *Structure*, 1999, **7**, 605–617.

5 P. Faller, B. Ctortecka, W. Tröger, T. Butz and M. Vašák, Optical and TDPAC spectroscopy of Hg(II)-rubredoxin: model for a mononuclear tetrahedral [Hg(CysS)$_4$]$^{2-}$ center, *J. Biol. Inorg. Chem.*, 2000, **5**, 393–401.

6 C.-C. Chang, L.-Y. Lin, X.-W. Zou, C.-C. Huang and N.-L. Chan, Structural basis of the mercury(II)-mediated conformational switching of the dual-function transcriptional regulator MerR, *Nucleic Acids Res.*, 2015, **43**, 7612–7623.

7 A. K. Wernimont, D. L. Huffman, A. L. Lamb, T. V. O'Halloran and A. C. Rosenzweig, Structural basis for copper transfer by the metallochaperone for the Menkes/Wilson disease proteins, *Nat. Struct. Biol.*, 2000, **7**, 766.

8 M. Łuczkowski, B. A. Zeider, A. V. H. Hinz, M. Stachura, S. Chakraborty, L. Hemmingsen, D. L. Huffman and V. L. Pecoraro, Probing the Coordination Environment of the Human Copper Chaperone HAH1: Characterization of HgII-Bridged Homodimeric Species in Solution, *Chem. – Eur. J.*, 2013, **19**, 9042–9049.

9 A. Changela, K. Chen, Y. Xue, J. Holschen, C. E. Outten, T. V. Halloran and A. Mondragón, Molecular Basis of Metal-Ion Selectivity and Zeptomolar Sensitivity by CueR, *Science*, 2003, **301**, 1383.

10 C. Ariöz, Y. Li and P. Wittung-Stafshede, The six metal binding domains in human copper transporter, ATP7B: molecular biophysics and disease-causing mutations, *Biometals*, 2017, **30**, 823–840.

11 P. A. Cobine, G. N. George, C. E. Jones, W. A. Wickramasinghe, M. Solioz and C. T. Dameron, Copper Transfer from the Cu(I) Chaperone, CopZ, to the Repressor, Zn(II)CopY: Metal Coordination Environments and Protein Interactions, *Biochemistry*, 2002, **41**, 5822–5829.

12 M. A. Kihlken, A. P. Leech and N. E. L. Brun, Copper-mediated dimerization of CopZ, a predicted copper chaperone from Bacillus subtilis, *Biochem. J.*, 2002, **368**, 729.

13 C. A. Blindauer and O. I. Leszczyszyn, Metallothioneins: unparalleled diversity in structures and functions for metal

ion homeostasis and more, *Nat. Prod. Rep.*, 2010, **27**, 720–741.

14 M. Capdevila, R. Bofill, Ò. Palacios and S. Atrian, State-of-the-art of metallothioneins at the beginning of the 21st century, *Coord. Chem. Rev.*, 2012, **256**, 46–62.

15 R. Bofill, M. Capdevila and S. Atrian, Independent metal-binding features of recombinant metallothioneins convergently draw a step gradation between Zn- and Cu-thioneins, *Metallomics*, 2009, **1**, 229–234.

16 M. Valls, R. Bofill, R. González-Duarte, P. González-Duarte, M. Capdevila and S. l. Atrian, A New Insight into Metallothionein (MT) Classification and Evolution: The in vivo and in vitro Metal Binding Features of Homarus Americanus Recombinant MT, *J. Biol. Chem.*, 2001, **276**, 32835–32843.

17 M. J. Stillman, Metallothioneins, *Coord. Chem. Rev.*, 1995, **144**, 461–511.

18 G. Henkel and B. Krebs, Metallothioneins: Zinc, Cadmium, Mercury, and Copper Thiolates and Selenolates Mimicking Protein Active Site Features – Structural Aspects and Biological Implications, *Chem. Rev.*, 2004, **104**, 801–824.

19 V. Calderone, B. Dolderer, H.-J. Hartmann, H. Echner, C. Luchinat, C. Del Bianco, S. Mangani and U. Weser, The crystal structure of yeast copper thionein: The solution of a long-lasting enigma, *Proc. Natl. Acad. Sci. U. S. A.*, 2005, **102**, 51–56.

20 L. Zhang, J. Pickering Ingrid, R. Winge Dennis and N. George Graham, X-Ray Absorption Spectroscopy of Cuprous-Thiolate Clusters in Saccharomyces cerevisiae Metallothionein, *Chem. Biodiversity*, 2008, **5**, 2042–2049.

21 M. J. Pushie, L. Zhang, I. J. Pickering and G. N. George, The fictile coordination chemistry of cuprous-thiolate sites in copper chaperones, *Biochim. Biophys. Acta, Bioenerg.*, 2012, **1817**, 938–947.

22 Z. Xiao, F. Loughlin, G. N. George, G. J. Howlett and A. G. Wedd, C-Terminal Domain of the Membrane Copper Transporter Ctr1 from Saccharomyces cerevisiae Binds Four Cu(I) Ions as a Cuprous-Thiolate Polynuclear Cluster: Sub-femtomolar Cu(I) Affinity of Three Proteins Involved in Copper Trafficking, *J. Am. Chem. Soc.*, 2004, **126**, 3081–3090.

23 J. A. Graden, M. C. Posewitz, J. R. Simon, G. N. George, I. J. Pickering and D. R. Winge, Presence of a Copper(I)–Thiolate Regulatory Domain in the Copper-Activated Transcription Factor Amt1, *Biochemistry*, 1996, **35**, 14583–14589.

24 X. Chen, H. Hua, K. Balamurugan, X. Kong, L. Zhang, G. N. George, O. Georgiev, W. Schaffner and D. P. Giedroc, Copper sensing function of Drosophila metal-responsive transcription factor-1 is mediated by a tetranuclear Cu(I) cluster, *Nucleic Acids Res.*, 2008, **36**, 3128–3138.

25 W. Lu, A. J. Zelazowski and M. J. Stillman, Mercury binding to metallothioneins: formation of the Hg_{18}-MT species, *Inorg. Chem.*, 1993, **32**, 919–926.

26 À. Leiva-Presa, M. Capdevila and P. Gonzàlez-Duarte, Mercury(II) binding to metallothioneins, *Eur. J. Biochem.*, 2004, **271**, 4872–4880.

27 O. Seneque, S. Crouzy, D. Boturyn, P. Dumy, M. Ferrand and P. Delangle, Novel model peptide for Atx1-like metallo-chaperones, *Chem. Commun.*, 2004, 770–771.

28 P. Rousselot-Pailley, O. Sénèque, C. Lebrun, S. Crouzy, D. Boturyn, P. Dumy, M. Ferrand and P. Delangle, Model Peptides Based on the Binding Loop of the Copper Metal-lochaperone Atx1: Selectivity of the Consensus Sequence MxCxxC for Metal Ions Hg(II), Cu(I), Cd(II), Pb(II), and Zn(II), *Inorg. Chem.*, 2006, **45**, 5510–5520.

29 A. Jancsó, B. Gyurcsik, E. Mesterházy and R. Berkecz, Competition of zinc(II) with cadmium(II) or mercury(II) in binding to a 12-mer peptide, *J. Inorg. Biochem.*, 2013, **126**, 96–103.

30 D. Szunyogh, B. Gyurcsik, F. H. Larsen, M. Stachura, P. W. Thulstrup, L. Hemmingsen and A. Jancsó, ZnII and HgII binding to a designed peptide that accommodates different coordination geometries, *Dalton Trans.*, 2015, **44**, 12576–12588.

31 E. Mesterházy, B. Boff, C. Lebrun, P. Delangle and A. Jancsó, Oligopeptide models of the metal binding loop of the bacterial copper efflux regulator protein CueR as potential Cu(I) chelators, *Inorg. Chim. Acta*, 2018, **472**, 192–198.

32 A. Jancsó, D. Szunyogh, F. H. Larsen, P. W. Thulstrup, N. J. Christensen, B. Gyurcsik and L. Hemmingsen, Towards the role of metal ions in the structural variability of proteins: CdII speciation of a metal ion binding loop motif, *Metallomics*, 2011, **3**, 1331–1339.

33 D. Szunyogh, H. Szokolai, P. W. Thulstrup, F. H. Larsen, B. Gyurcsik, N. J. Christensen, M. Stachura, L. Hemmingsen and A. Jancsó, Specificity of the Metalloregulator CueR for Monovalent Metal Ions: Possible Functional Role of a Coordinated Thiol?, *Angew. Chem., Int. Ed.*, 2015, **54**, 15756–15761.

34 S. Chakraborty, J. Yudenfreund Kravitz, P. W. Thulstrup, L. Hemmingsen, W. F. DeGrado and V. L. Pecoraro, Design of a Three-Helix Bundle Capable of Binding Heavy Metals in a Triscysteine Environment, *Angew. Chem., Int. Ed.*, 2011, **50**, 2049–2053.

35 O. Iranzo, P. W. Thulstrup, S.-b. Ryu, L. Hemmingsen and V. L. Pecoraro, The Application of ^{199}Hg NMR and ^{199m}Hg Perturbed Angular Correlation (PAC) Spectroscopy to Define the Biological Chemistry of HgII: A Case Study with Designed Two- and Three-Stranded Coiled Coils, *Chem. – Eur. J.*, 2007, **13**, 9178–9190.

36 A.-S. Jullien, C. Gateau, C. Lebrun and P. Delangle, Mercury Complexes with Tripodal Pseudopeptides Derived from d-Penicillamine Favour a HgS_3 Coordination, *Eur. J. Inorg. Chem.*, 2015, 3674–3680.

37 A. M. Pujol, C. Lebrun, C. Gateau, A. Manceau and P. Delangle, Mercury-Sequestering Pseudopeptides with a Tris(cysteine) Environment in Water, *Eur. J. Inorg. Chem.*, 2012, 3835–3843.

38 A.-S. Jullien, C. Gateau, C. Lebrun, I. Kieffer, D. Testemale and P. Delangle, D-Penicillamine Tripodal Derivatives as Efficient Copper(I) Chelators, *Inorg. Chem.*, 2014, **53**, 5229–5239.

39 A. M. Pujol, C. Gateau, C. Lebrun and P. Delangle, A Series of Tripodal Cysteine Derivatives as Water-Soluble Chelators that are Highly Selective for Copper(I), *Chem. – Eur. J.*, 2011, **17**, 4418–4428.

40 O. Sénèque, P. Rousselot-Pailley, A. Pujol, D. Boturyn, S. Crouzy, O. Proux, A. Manceau, C. Lebrun and P. Delangle, Mercury Trithiolate Binding (HgS₃) to a de Novo Designed Cyclic Decapeptide with Three Preoriented Cysteine Side Chains, *Inorg. Chem.*, 2018, **57**, 2705–2713.

41 M. Imagawa, T. Onozawa, K. Okumura, S. Osada, T. Nishihara and M. Kondo, Characterization of metallothionein cDNAs induced by cadmium in the nematode Caenorhabdita elegans, *Biochem. J.*, 1990, **268**, 237.

42 S. Perez-Rafael, A. Kurz, M. Guirola, M. Capdevila, O. Palacios and S. Atrian, Is MtnE, the fifth Drosophila metallothionein, functionally distinct from the other members of this polymorphic protein family?, *Metallomics*, 2012, **4**, 342–349.

43 D. R. Winge, K. B. Nielson, W. R. Gray and D. H. Hamer, Yeast metallothionein. Sequence and metal-binding properties, *J. Biol. Chem.*, 1985, **260**, 14464–14470.

44 M. Vasak, J. H. R. Kaegi and H. A. O. Hill, Zinc(ɪɪ), cadmium(ɪɪ), and mercury(ɪɪ) thiolate transitions in metallothionein, *Biochemistry*, 1981, **20**, 2852–2856.

45 P. Faller, Neuronal growth-inhibitory factor (metallothionein-3): reactivity and structure of metal–thiolate clusters, *FEBS J.*, 2010, **277**, 2921–2930.

46 A. Presta, A. R. Green, A. Zelazowski and M. J. Stillman, Copper Binding to Rabbit Liver Metallothionein, *Eur. J. Biochem.*, 1995, **227**, 226–240.

47 E. Kaiser, R. L. Colescott, C. D. Bossinger and P. I. Cook, Color test for detection of free terminal amino groups in the solid-phase synthesis of peptides, *Anal. Biochem.*, 1970, **34**, 595–598.

48 P. Kamau and R. B. Jordan, Complex Formation Constants for the Aqueous Copper(ɪ)–Acetonitrile System by a Simple General Method, *Inorg. Chem.*, 2001, **40**, 3879–3883.

49 G. L. Ellman, Tissue sulfhydryl groups, *Arch. Biochem. Biophys.*, 1959, **82**, 70–77.

50 P. W. Riddles, R. L. Blakeley and B. Zerner, *Methods Enzymol.*, 1983, **91**, 49–60.

51 Z. Xiao, J. Brose, S. Schimo, S. M. Ackland, S. La Fontaine and A. G. Wedd, Unification of the Copper(ɪ) Binding Affinities of the Metallo-chaperones Atx1, Atox1, and Related Proteins: Detection Probes and Affinity Standards, *J. Biol. Chem.*, 2011, **286**, 11047–11055.

52 H. Gampp, M. Maeder, C. J. Meyer and A. D. Zuberbühler, Calculation of equilibrium constants from multiwavelength spectroscopic data—I, *Talanta*, 1985, **32**, 95–101.

53 H. Gampp, M. Maeder, C. J. Meyer and A. D. Zuberbühler, Calculation of equilibrium constants from multiwavelength spectroscopic data—II, *Talanta*, 1985, **32**, 257–264.

54 H. Gampp, M. Maeder, C. J. Meyer and A. D. Zuberbühler, Calculation of equilibrium constants from multiwavelength spectroscopic data—III, *Talanta*, 1985, **32**, 1133–1139.

55 H. Gampp, M. Maeder, C. J. Meyer and A. D. Zuberbühler, Calculation of equilibrium constants from multiwavelength spectroscopic data—IV, *Talanta*, 1986, **33**, 943–951.

56 L. G. Sillen, Electrometric Investigation of Equilibria between Mercury and Halogen Ions. Vlll. Survey and Conclusions, *Acta Chem. Scand.*, 1949, **3**, 539–553.

57 I. Grenthe, A. V. Plyasunov and K. Spahiu, *Estimations of Medium Effects on Thermodynamic Data*, in *Modelling in aquatic chemistry*, ed. I. Grenthe and I. Puigdomenech, OECD Publications, 1997, ch. IX, pp. 325–426.

58 J. Powell Kipton, L. Brown Paul, H. Byrne Robert, T. Gajda, G. Hefter, S. Sjöberg and H. Wanner, Chemical speciation of environmentally significant heavy metals with inorganic ligands. Part 1: The Hg²⁺, Cl⁻, OH⁻, CO₃²⁻, SO₄²⁻, and PO₄³⁻ aqueous systems, *Pure Appl. Chem.*, 2005, **77**, 739.

59 L. Zékány, I. Nagypál and G. Peintler, *PSEQUAD for chemical equilibria*, Technical Software Distributors, Baltimore, MD, 1991.

60 R. Brooks Bernard, E. Bruccoleri Robert, D. Olafson Barry, J. States David, S. Swaminathan and M. Karplus, CHARMM: A program for macromolecular energy, minimization, and dynamics calculations, *J. Comput. Chem.*, 1983, **4**, 187–217.

61 A. D. Becke, Density-functional exchange-energy approximation with correct asymptotic behavior, *Phys. Rev. A: At., Mol., Opt. Phys.*, 1988, **38**, 3098–3100.

62 C. Lee, W. Yang and R. G. Parr, Development of the Colle-Salvetti correlation-energy formula into a functional of the electron density, *Phys. Rev. B: Condens. Matter Mater. Phys.*, 1988, **37**, 785–789.

63 A. D. Becke, Density-functional thermochemistry. III. The role of exact exchange, *J. Chem. Phys.*, 1993, **98**, 5648–5652.

64 (a) M. J. Frisch, G. W. Trucks, H. B. Schlegel, G. E. Scuseria, M. A. Robb, J. R. Cheeseman, V. G. Zakrzewski, J. A. Montgomery Jr., R. E. Stratmann, J. C. Burant, S. Dapprich, J. M. Millam, A. D. Daniels, K. N. Kudin, M. C. Strain, O. Farkas, J. Tomasi, V. Barone, M. Cossi, R. Cammi, B. Mennucci, C. Pomelli, C. Adamo, S. Clifford, J. Ochterski, G. A. Petersson, P. Y. Ayala, Q. Cui, K. Morokuma, N. Rega, P. Salvador, J. J. Dannenberg, D. K. Malick, A. D. Rabuck, K. Raghavachari, J. B. Foresman, J. Cioslowski, J. V. Ortiz, A. G. Baboul, B. B. Stefanov, G. Liu, A. Liashenko, P. Piskorz, I. Komaromi, R. Gomperts, R. L. Martin, D. J. Fox, T. Keith, M. A. Al-Laham, C. Y. Peng, A. Nanayakkara, M. Challacombe, P. M. W. Gill, B. Johnson, W. Chen, M. W. Wong, J. L. Andres, C. Gonzalez, M. Head-Gordon, E. S. Replogle and J. A. Pople, *Gaussian 98, revision A.11.3*, Gaussian, Inc., Pittsburgh, PA, 2002; (b) M. J. Frisch, *et al.*, *Gaussian03*.

65 F. Šebesta, V. Sláma, J. Melcr, Z. Futera and J. V. Burda, Estimation of Transition-Metal Empirical Parameters for Molecular Mechanical Force Fields, *J. Chem. Theory Comput.*, 2016, **12**, 3681–3688.

66 L. Themis and K. Martin, Effective energy function for proteins in solution, *Proteins: Struct., Funct., Bioinf.*, 1999, **35**, 133–152.

67 P. Dumy, I. M. Eggleston, G. Esposito, S. Nicula and M. Mutter, Solution structure of regioselectively addressable functionalized templates: An NMR and restrained molecular dynamics investigation, *Biopolymers*, 1996, **39**, 297–308.

68 A. M. Pujol, M. Cuillel, O. Renaudet, C. Lebrun, P. Charbonnier, D. Cassio, C. Gateau, P. Dumy, E. Mintz and P. Delangle, Hepatocyte Targeting and Intracellular

Copper Chelation by a Thiol-Containing Glycocyclopeptide, *J. Am. Chem. Soc.*, 2011, **133**, 286–296.

69 C. S. Bonnet, P. H. Fries, S. Crouzy, O. Sénèque, F. Cisnetti, D. Boturyn, P. Dumy and P. Delangle, A Gadolinium-Binding Cyclodecapeptide with a Large High-Field Relaxivity Involving Second-Sphere Water, *Chem. – Eur. J.*, 2009, **15**, 7083–7093.

70 M. Beltramini and K. Lerch, Spectroscopic studies on Neurospora copper metallothionein, *Biochemistry*, 1983, **22**, 2043–2048.

71 A. M. Pujol, C. Gateau, C. Lebrun and P. Delangle, A Cysteine-Based Tripodal Chelator with a High Affinity and Selectivity for Copper(I), *J. Am. Chem. Soc.*, 2009, **131**, 6928–6929.

72 C. T. Dameron, D. R. Winge, G. N. George, M. Sansone, S. Hu and D. Hamer, A copper-thiolate polynuclear cluster in the ACE1 transcription factor, *Proc. Natl. Acad. Sci. U. S. A.*, 1991, **88**, 6127–6131.

73 D. L. Pountney, I. Schauwecker, J. Zarn and M. Vasak, Formation of Mammalian Cu_8-Metallothionein in vitro: Evidence for the Existence of Two $Cu(I)_4$-Thiolate Clusters, *Biochemistry*, 1994, **33**, 9699–9705.

74 S. M. Kelly and N. C. Price, The Use of Circular Dichroism in the Investigation of Protein Structure and Function, *Curr. Protein Pept. Sci.*, 2000, **1**, 349–384.

75 Y. J. Li and U. Weser, Circular dichroism, luminescence, and electronic absorption of copper binding sites in metallothionein and its chemically synthesized alpha. and beta domains, *Inorg. Chem.*, 1992, **31**, 5526–5533.

76 A.-S. Jullien, C. Gateau, I. Kieffer, D. Testemale and P. Delangle, X-ray Absorption Spectroscopy Proves the Trigonal-Planar Sulfur-Only Coordination of Copper (I) with High-Affinity Tripodal Pseudopeptides, *Inorg. Chem.*, 2013, **52**, 9954–9961.

77 E. Mesterházy, C. Lebrun, A. Jancsó and P. Delangle, A Constrained Tetrapeptide as a Model of Cu(I) Binding Sites Involving Cu_4S_6 Clusters in Proteins, *Inorg. Chem.*, 2018, **57**, 5723–5731.

78 R. G. Pearson, Hard and Soft Acids and Bases, *J. Am. Chem. Soc.*, 1963, **85**, 3533–3539.

79 M. Łuczkowski, M. Stachura, V. Schirf, B. Demeler, L. Hemmingsen and V. L. Pecoraro, Design of Thiolate Rich Metal Binding Sites within a Peptidic Framework, *Inorg. Chem.*, 2008, **47**, 10875–10888.

80 G. R. Dieckmann, D. K. McRorie, D. L. Tierney, L. M. Utschig, C. P. Singer, T. V. O'Halloran, J. E. Penner-Hahn, W. F. DeGrado and V. L. Pecoraro, De Novo Design of Mercury-Binding Two- and Three-Helical Bundles, *J. Am. Chem. Soc.*, 1997, **119**, 6195–6196.

81 S. Pires, J. Habjanič, M. Sezer, C. M. Soares, L. Hemmingsen and O. Iranzo, Design of a Peptidic Turn with High Affinity for HgII, *Inorg. Chem.*, 2012, **51**, 11339–11348.

82 J. S. Casas and M. M. Jones, Mercury(II) complexes with sulfhydryl containing chelating agents: Stability constant inconsistencies and their resolution, *J. Inorg. Nucl. Chem.*, 1980, **42**, 99–102.